

# **A spinodal decomposition model for the large-scale structure of the universe**

Nitish Yadav\*

*K. R. Mangalam University, Gurugram (India)*

*\*email: nitishyadav.ny@gmail.com*

## **Abstract**

The tremendous efforts placed in understanding the structure and galaxy formation in the universe have led to major improvements in our models for the universe. Particular the computational simulations that solve its non-linear growth have painted a clearer picture of the processes behind the enormous scale and shape of the structures observed experimentally. Inspired by porous structure of polymer membranes prepared using phase-inversion, we have taken a fresh-approach to understand how the universe got its present structure. We present the results of a finite-element method based simulation to predict large-scale structure formation in the universe. The novel method applies the Cahn-Hilliard model of spinodal decomposition of a binary mixture to predict the dynamics of matter and dark-energy distribution in the universe. The results closely match the various surveys of matter distribution in the universe and can prove to be an important step towards decreasing the computational resources required for future simulations.

## **Keywords**

Large-scale structure; dark-matter; dark-energy; spinodal-decomposition; finite-element method

## **Introduction**

Predicting the large-scale structure of the universe using computational models provides a robust means to compare with experimental results, leading to important insights about the interactions and physical laws that govern its evolution and evaluate the validity of existing theories. These N-body

calculations employ numerical techniques to simulate the evolution of structures involving normal and dark-matter, and dark-energy. Since much is unknown about the nature of dark-matter and dark-energy the simulations allow for validation of theoretical models about them. A number of important studies have reported results of simulations that involving huge number of interacting particles (e.g.  $\sim 10^6$  for the Millenium simulation<sup>1</sup> in large volumes.<sup>2-9</sup> Much of these numerical simulations are based on interactions between particles and their subsequent motion in space, and are computationally expensive. A novel approach that can provide a fresh perspective to look at the universe's evolution and at the same time also reduce the computational time may lead to greater progress in the field.

While the laws of physics such as general relativity, or forces such as gravity, that are valid for the cosmic length scale are not applicable on the very small length scales. However, it can be safely assumed that the thermodynamic differential equations that are applicable on one length scale should hold very well for the other, whether be it the large-scale structure of our universe, or a binary mixture such as that of a polymer in a solvent. The thermodynamics and kinetics of polymer solutions is a intriguing topic from many aspects. The complex structure of polymers and the interaction with the solvent/non-solvent lead to phase-separation and crystallization. These processes can be explained using binary phase diagrams in case of a two component (polymer - solvent) system, and by ternary phase diagram for a three component (polymer – solvent – non-solvent system). The phase separation process is associated with the formation of polymer-rich and polymer-poor regions in the solution, ultimately leading to porous membranes. The porous structure of a membrane is determined by the initial solution composition, the phase-inversion rate and the interactions between the components of the solution.<sup>10,11</sup>

Broadly, phase-separation methods are of two types. The first is the non-solvent induced phase separation (NIPS) method where a non-solvent (with respect to the polymer) is introduced in the

polymer - solvent system. The non-solvent penetrates the polymer-solvent solution and causes the formation of polymer-rich and polymer-poor (non-solvent rich) regions. This is followed by diffusion of solvent ions from the polymer rich phase to the non-solvent rich regions, leading to precipitation of the polymer-rich regions into solid polymeric walls and filaments around the polymer-poor voids, as shown in **Fig. 1(a)**.

The second process is the thermally induced phase separation (TIPS) method for a binary system of polymer and solvent. This process is characterized by a decrease in polymer-solvent interaction as the temperature of the system is reduced, leading to liquid-liquid demixing (a polymer-rich phase and a polymer-poor phase). A typical porous membrane prepared using TIPS is shown in **Fig. 1(b)**. Further, as depicted in **Fig. 1(c)**, the initial solution concentration determines the fate of the final polymeric structure, i.e., whether we obtain polymer rich spheroids, a spinodal decomposition leading to bi-continuous porous structure where the pores/voids as well as a the polymer rich regions both are connected throughout the material, or a porous structure where the pores are completely enclosed by the polymeric walls.<sup>11</sup>

In the present work we show that the evolution of the large-scale structure of the universe can be explained by the same thermodynamical differential equation that govern a polymer-solvent system undergoing the TIPS process. A polymer solution undergoing spinodal diffusion forms a porous microstructure if its initial composition lies within the spinodal region (Fig. 1c). Also, we know that the universe has matter dominated filaments and dark-energy dominated voids. Therefore, if a binary phase-diagram could be drawn for the universe, it would be safe to assume currently inside the spinodal curve and moving towards coarsening (Oswald ripening) of the voids and filaments.

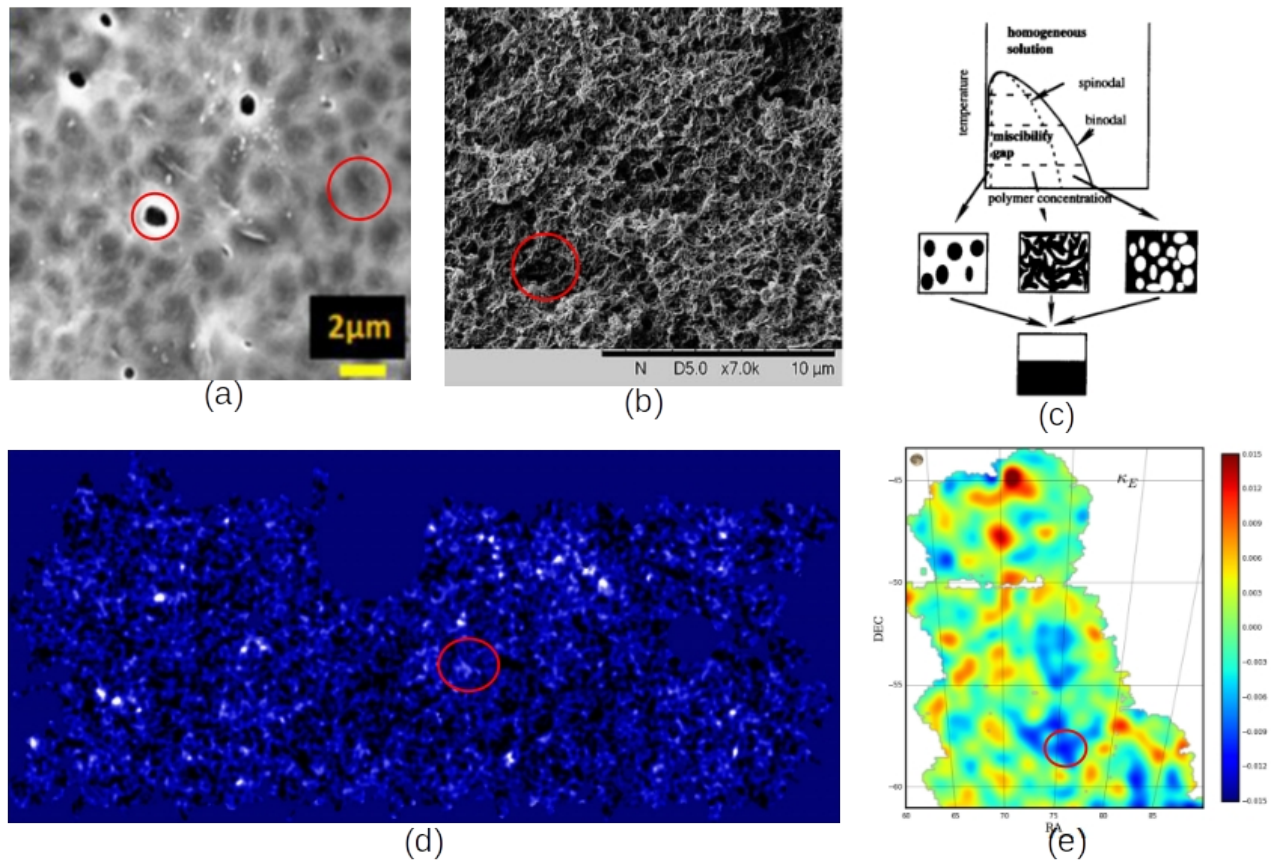


**Figure 1.** Scanning electron micrograph of a polymer membrane prepared by (a) the non-solvent induced phase separation (NIPS) method, (b) the thermally induced phase separation (TIPS) method, (c) diagram showing the spinodal region for a binary polymer-solvent solution and the resulting polymer membrane morphologies, dependent on the initial solution composition. (d) The large-scale structure of the universe as observed by the Subaru/Suprime Cam Survey, and (e) the large-scale structure as observed by the Dark Energy Survey. Red circles have been superimposed to highlight the voids in each case. Image courtesy: Yadav et al.<sup>12</sup>, Pan et al.<sup>13</sup>, Witte et al.<sup>11</sup>, Oguri et al.<sup>14</sup>, Vikram et al.<sup>15</sup>

## Methodology

For the finite-element calculations we have used the open-source python package DOLFINx along with the Unified Form Language package (UFL).<sup>16,17</sup> For the initial system state, we have used a 128 bit seed to generate uniformly random distribution of noise in the initial concentration ( $c_0 = 0.316$ ). The calculations have been performed using a  $100 \times 100$  mesh for 500 time step sizes with

variation in the free energy coefficient and the time-step size. The matter distribution maps have been made using ParaView software.<sup>18</sup>

## Results and Discussion

**Fig. 1(d)** shows the two-dimensional wide-field, weak-lensing total mass map using the Hyper Suprime-Cam Subaru Strategic program data.<sup>14</sup> **Fig. 1(e)** shows the part of the large-scale structure of our universe as determined by the Dark Energy Survey (DES).<sup>15</sup> The analogy between the large-scale structure of the universe and the porous morphology of polymer membranes obtained by the TIPS and NIPS methods is striking.

In the remainder of this article, the authors argue that the processes determining the evolution of the voids and galactic filaments are analogous to the TIPS methods. Despite the similarities in the morphology, we do not discuss the NIPS method as it involves a third component (the non-solvent) which doesn't seem to have any direct analogue in the theories of the large-scale structure. On the other hand, like the TIPS methods, the cooling down of the universe might have led to a demixing between the initially homogenous distribution of matter/dark matter (the polymer) and dark energy (the solvent). A polymer dissolves completely in the solvent at high temperatures, but the change in the Gibbs free energy allows it the system to separate into a polymer-rich phase and a polymer-poor phase when cooled below a certain threshold temperature. Similarly, matter might have started to undergo 'phase-separation' when the temperature of the early universe dropped below a threshold value (due to expansion of space). The formation of the voids could have begun as the decomposition into the matter-poor and matter-rich phases progressed. The voids would then have become dominated by dark-energy, similar to the pores (voids) in the TIPS process becoming solvent-rich. The matter-rich part could then coagulate to form the filaments (and walls) between these dark-energy filled voids. This suggests that there may be a similar mathematical model for the void formation in polymer solutions and the early universe. The Cahn-Hilliard model successfully

explains structure formation (voids, walls and filaments) via thermally induced spinodal decomposition in a binary mixture. We attempt to apply this same model to the early universe to try and model distribution of matter in it. The Cahn-Hilliard equation is a parabolic equation and involves first-order time derivatives, and second- and fourth-order spatial derivatives.

This equation, proposed by Cahn<sup>19</sup> for spinodal decomposition in a polymer solution can be derived by considering the free energy as a function of the local free energy of mixing ( $f(c)$ ) and the concentration gradient  $\nabla(c)$ .

$$G(c) = \int_V [f(c) + \kappa(\nabla c)^2] d\mathbf{r} \quad \dots (1)$$

where  $\kappa$  is called the gradient energy coefficient.

The concentration gradient term arises due the diffuse nature of the interface between pores (voids) and the polymer-rich domains. The chemical potential of the polymer ( $\mu_1$ ) and solvent ( $\mu_2$ ) and the diffusional flux are related by a mobility term  $M(c)$

$$M(c) = \frac{J}{\mu_2 - \mu_1} \quad \dots (2)$$

Further, the mobility difference can be found by minimizing the free energy difference in equation (1) with respect to  $c$  at the interface. This is done by assuming that the average concentration in space remains constant, i.e. if  $c_0$  is the initial concentration the polymer, then

$$\int_V (c - c_0) d\mathbf{r} = 0 \quad \dots (3)$$

leading to

$$\mu_2 - \mu_1 = \frac{\partial f}{\partial c} - 2\kappa \nabla^2 c \quad \dots (4)$$

Finally, to find the differential equation governing the spinodal decomposition process, we use the differential mass balance condition for an infinitesimal volume of space

$$\frac{\partial c}{\partial t} = -\nabla \cdot \mathbf{J} \quad \dots (5)$$

Replacing the definition of  $J$  from equation (2) and that of  $\mu_2 - \mu_1$  from equation (4), equation (5) becomes

$$\frac{\partial c}{\partial t} = \nabla \cdot \left[ M(c) \nabla \left[ \left( \frac{\partial f}{\partial c} \right) - 2\kappa \nabla^2 c \right] \right] \quad \dots (6)$$

This non-linear equation (6) can be solved numerically using the finite element method and the time evolution of the spinodal decomposition observed.

Additionally, for the early stages of spinodal decomposition, equation (6) can also be linearized using the average composition of the solution  $c_0$ , i.e. if we assume that  $M(c) \approx M_0 c$ , with  $M_0$  evaluated at the average composition  $c_0$ . This approximation leads to the following linearized form of the differential equation

$$\frac{\partial c}{\partial t} = M_0 \left[ \left( \frac{\partial^2 f}{\partial^2 c} \right)_0 \nabla^2 c - 2\kappa \nabla^4 c \right] \quad \dots (7)$$

where, just like  $M_0$ ,  $\left( \frac{\partial^2 f}{\partial^2 c} \right)_0$  too is evaluated at the average composition  $c_0$ . The analytical solution of equation (7) valid only in the early stages of decomposition is given as

$$c = c_0 + \sum_{\mathbf{K}} \exp[r(\mathbf{K})t] [A(\mathbf{K}) \cos(\mathbf{K} \cdot \mathbf{r}) + B(\mathbf{K}) \sin(\mathbf{K} \cdot \mathbf{r})] \quad \dots (8)$$

with

$$r(\mathbf{k}) = - \left[ M_0 \left( \frac{\partial^2 f}{\partial^2 c} \right)_0 (\mathbf{K} \cdot \mathbf{K}) + 2M_0 \kappa (\mathbf{K} \cdot \mathbf{K})^2 \right] \quad \dots (9)$$

where  $\mathbf{K}$  is the fluctuation wavevector. Fig. 2 depicts the typical growth of high and low concentration regions as the system evolves starting from a homogeneous solution with minor sinusoidal perturbations. The growth of structures, however, is more or less independent of the type of initial perturbations in the system. Even for random fluctuations in the concentration, the system eventually progresses in a similar manner. The coagulated nature of matter in the large-scale

structure of the universe can be explained as a result of these density fluctuations in the Cahn-Hilliard model. The resonant wavelength (  $\lambda_m$  ) of the most rapidly growing peak is found to be

$$\lambda_m = 2(2^{\frac{1}{2}})\pi \left[ -\frac{\left(\frac{\partial^2 f}{\partial^2 c}\right)_0}{2\kappa} \right] \dots (10)$$

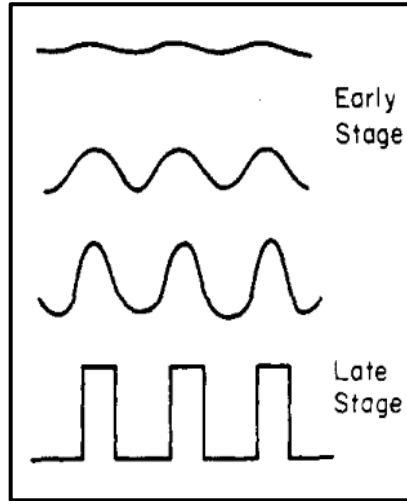


**Figure 2.** Density fluctuations in a polymer-solution during the thermally induced phase-separation process. (Image courtesy: Caneba et al.<sup>10</sup>)

For the present work we apply the non-linear equation (6) to the early universe. The concentration and temperature dependent mobility term  $M(c)$  can be modified to effect the final distribution of matter and dark energy in our calculations. The thickness of the walls and the filaments when compared with the present experiment evidence must give an estimate of the form of  $M(c)$ , among other initial conditions, the early universe might have had. For example, the Huston-Cahn-Hilliard model assumed the following form for  $M(c)$ <sup>20</sup>

$$M(c) = \frac{c(1-c)}{RT} [D_1 c + D_2 (1-c)] \dots (11)$$

here  $D_1$  and  $D_2$  are the self-diffusivities of the polymer and solvent phase, respectively. Alternatively, we may begin the numerical calculations by approximating both  $M$  and  $D$  as polynomial functions in  $c$ .



The matter distribution at different times ( $t$ ) are shown in **Fig. 3 – 5**. We have used a 2-dimensional finite element mesh to perform matter transport simulations using equation (6). We expect the initial state of the system to correspond to a point inside the spinodal curve on the binary phase diagram. Therefore, even slight fluctuations (in-homogeneity) in the matter distribution (concentration) are expected to lead to spinodal decomposition. We impose a slight random fluctuation around the mean concentration value to initiate the decomposition. The time step size and total number of time steps are  $5 \times 10^{-6}$  and 500, respectively, for the results shown in Fig. 3, and  $5 \times 10^{-8}$  and 500 for results shown in Fig. 4. We have avoided assigning any specific unit to time due to the abstract definition of our system. The local free energy  $f(c)$  is approximated by a fourth order polynomial. The gradient energy coefficient  $\kappa$  has been fixed at  $10^{-2}$ . The initial concentration of the total matter (normal and dark) has been taken as 31.7 % (4.9 % normal matter, 26.8 % dark matter), and 68.3 % dark energy, as per the latest results by the Planck space telescope project.<sup>21,22</sup> The variation in the form and the parameters of the mobility factor  $M(c)$  result in different matter distributions at the end of each simulation. We find that when  $M(c)$  is approximated by equation (11) (with the matter and dark energy diffusivity and temperature ratios taken as  $D_1/RT = 0.01$  and  $D_2/RT = 0.1$ , respectively). The local free energy density has been taken as  $f(c) = 100c^2(1-c)^2$  for Fig. 3 and  $f(c) = 1000c^2(1-c)^2$  for the results in Fig. 4. The final matter – dark-energy energy distributions provide results comparable to experimental observations reported by the various experimental surveys of dark-matter and dark-energy (**Fig. 1d, Fig. 1e, Fig. 5a and 5b**).

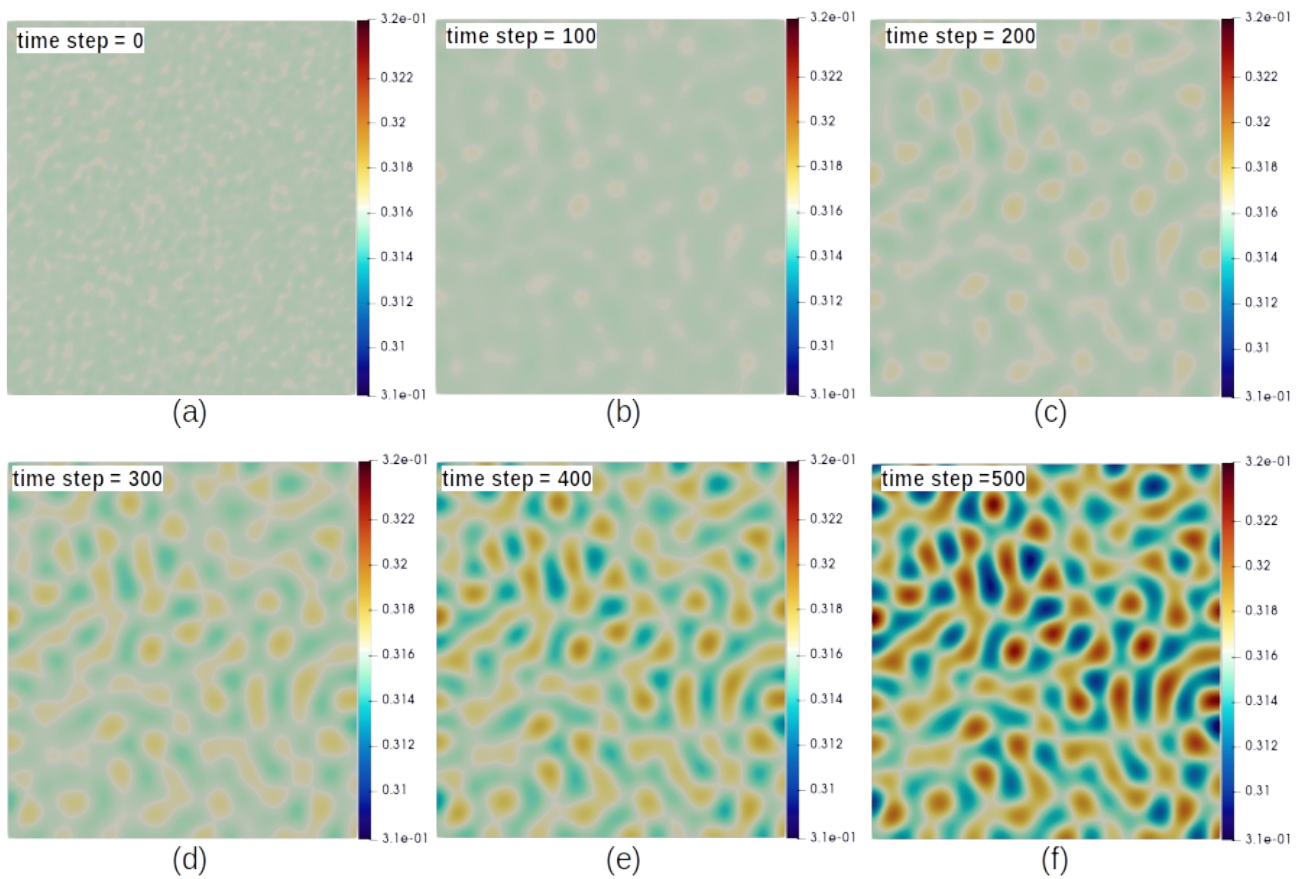


**Figure 3 .** The results of the 2-D Cahn-Hilliard simulation using the finite element method. (a) The initial distribution of mass for the simulation. (b-d) the gradual spinodal decomposition of the matter – dark-energy system into matter-rich (red) and dark-energy (blue) regions. The matter-rich phase is concentrated in well-defined regions, as expected from the solution of the Cahn-Hilliard equation.

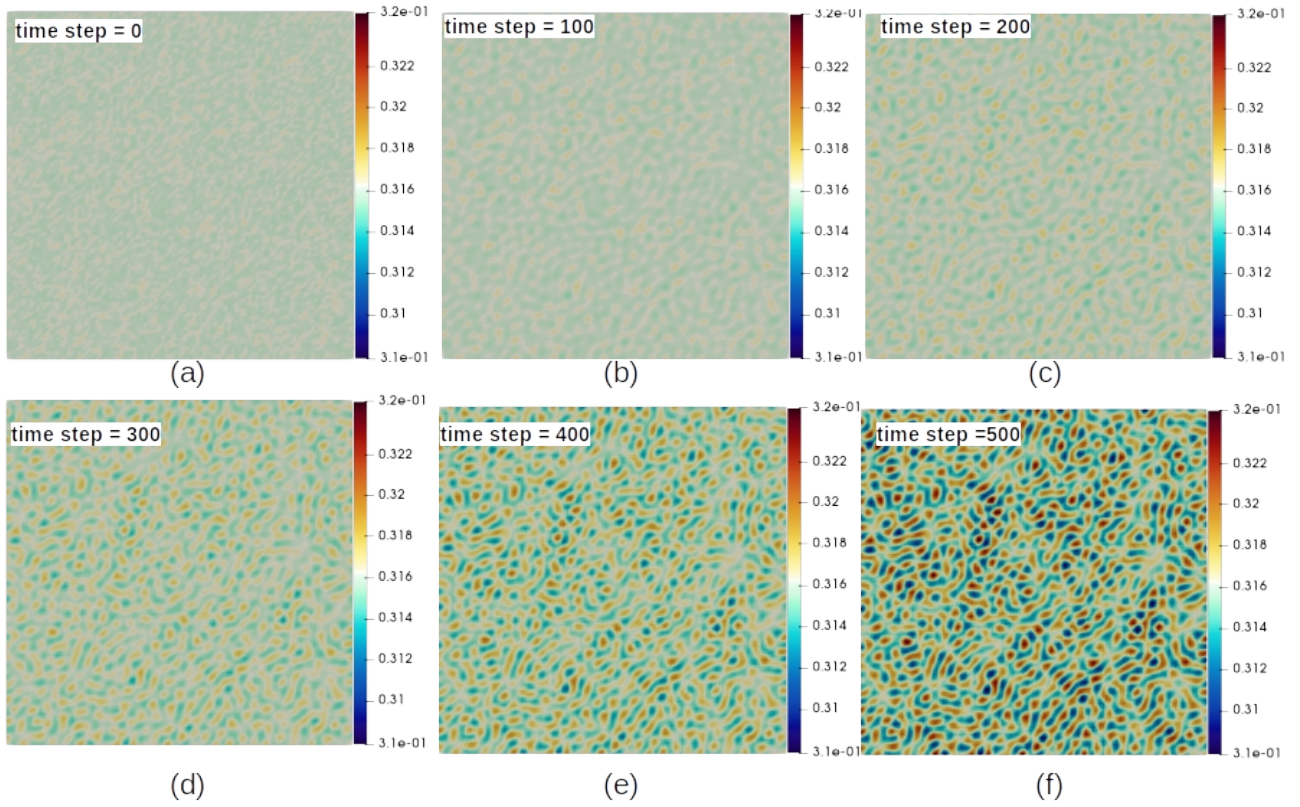


**Figure 4** . Same as Figure 3, expect the form of local free energy density is

$$f(c) = 1000c^2(1-c)^2 \quad \text{and time step size is } 5 \times 10^{-8}.$$

Fig. 5(a) shows the weak lensing mass map (E-band convergence  $\kappa_E$  map, showing pixel signal-to-noise ( $S/N$ ) ( $\kappa_E / \sigma(\kappa_E)$ ) in the redshift range of  $0.2 < z < 1.3$ . The METACALIBRATION catalogue for galaxies was used to construct this map.<sup>23</sup> Fig. 5(b) shows the mass distribution convergence in the galaxy cluster Cl0023+1654 at  $z = 0.395$ , reconstructed using the weak-lensing data from Subaru Suprime-Cam instrument survey.<sup>24</sup> The clear similarities between the finite-element calculations in this work and the experimental observations in Fig. 5 indicate that the spinodal-decomposition model can be effectively used to simulate the evolution of matter distribution for a wide range of redshift. Additionally, Newtonian or relativistic interactions have not been used to arrive at any of the results in the current work. Therefore, using the spinodal-decomposition method with these traditional simulations can lead to increasing the efficiency of the traditional algorithms, decrease the computation time, and provide innovative insights into the processes that lead to emergence and growth of structures in our universe.

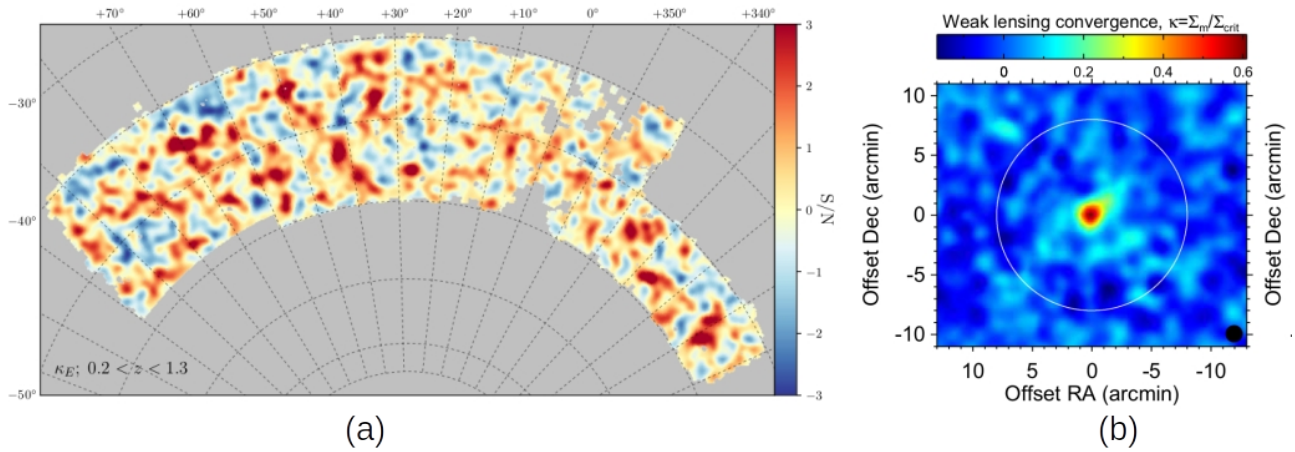


**Figure 5.** Weak lensing data map from the (a) Dark Energy Survey and (b) from the Subaru/Suprime-Cam survey (Image courtesy:(a) Chang et al.<sup>23</sup> (b) Umetsu et al.<sup>24</sup>)

## Conclusion

Thermally induced phase-separation in binary mixtures such as polymer-solvent system lead to porous morphologies similar to the current large-scale structure of the universe. The use of the Cahn-Hilliard model for spinodal decomposition provides reasonable matter distribution plots that look very similar to those observed experimentally. Using this model to estimate the large-scale structure of the universe could allow us to gain fundamental insights into the evolution of the universe, lead to potentially useful new numerical methods, and reduce the amount of computational resources needed to carry out similar tasks.

## Acknowledgement

Nitish Yadav would like to acknowledge K. R. Mangalam University for providing support in conducting research.

## References

1. Springel, V. *et al.* Simulating the joint evolution of quasars, galaxies and their large-scale distribution. *Nature* **435**, 629–636 (2005).
2. Schaye, J. *et al.* The FLAMINGO project: cosmological hydrodynamical simulations for large-scale structure and galaxy cluster surveys. *Monthly Notices of the Royal Astronomical Society* **526**, 4978–5020 (2023).
3. Centrella, J. & Melott, A. L. Three-dimensional simulation of large-scale structure in the universe. *Nature* **305**, 196–198 (1983).
4. Frenk, C. S., White, S. D. & Davis, M. Nonlinear evolution of large-scale structure in the universe. *Astrophysical Journal, Part 1 (ISSN 0004-637X)*, vol. 271, Aug. 15, 1983, p. 417-430. **271**, 417–430 (1983).
5. Klypin, A. A. & Shandarin, S. F. Three-dimensional numerical model of the formation of large-scale structure in the Universe. *Monthly Notices of the Royal Astronomical Society* **204**, 891–907 (1983).
6. Doroshkevich, A. G. *et al.* Two-dimensional simulation of the gravitational system dynamics and formation of the large-scale structure of the universe. *Monthly Notices of the Royal Astronomical Society* **192**, 321–337 (1980).
7. Crain, R. A. & Van De Voort, F. Hydrodynamical Simulations of the Galaxy Population: Enduring Successes and Outstanding Challenges. *Annual Review of Astronomy and Astrophysics* **61**, 473–515 (2023).
8. Ivanov, M. M. *et al.* Constraining early dark energy with large-scale structure. *Phys. Rev. D* **102**, 103502 (2020).
9. Angulo, R. E. *et al.* The BACCO simulation project: exploiting the full power of large-scale structure for cosmology. *Monthly Notices of the Royal Astronomical Society* **507**, 5869–5881 (2021).
10. Caneba, G. T. & Soong, D. S. Polymer membrane formation through the thermal-inversion process. 2. Mathematical modeling of membrane structure formation. *Macromolecules* **18**,

2545–2555 (1985).

11. van de Witte, P., Dijkstra, P. J., van den Berg, J. W. A. & Feijen, J. Phase separation processes in polymer solutions in relation to membrane formation. *Journal of Membrane Science* **117**, 1–31 (1996).
12. Yadav, N., Mishra, K. & Hashmi, S. A. Nanozirconia polymer composite porous membrane prepared by sustainable immersion precipitation method for use as electrolyte in flexible supercapacitors. *Materials Today Communications* **25**, 101506 (2020).
13. Pan, J., Xiao, C., Huang, Q., Wang, C. & Liu, H. Fabrication and properties of poly (ethylene chlorotrifluoroethylene) membranes via thermally induced phase separation (TIPS). *RSC Advances* **5**, 45249–45257 (2015).
14. Oguri, M. *et al.* Two-and three-dimensional wide-field weak lensing mass maps from the Hyper Suprime-Cam Subaru Strategic Program S16A data. *Publications of the Astronomical Society of Japan* **70**, S26 (2018).
15. Vikram, V. *et al.* Wide-field lensing mass maps from Dark Energy Survey science verification data: Methodology and detailed analysis. *Phys. Rev. D* **92**, 022006 (2015).
16. Baratta, I. A. *et al.* DOLFINx: The next generation FEniCS problem solving environment. Preprint at <https://doi.org/10.5281/zenodo.10447666> (2023).
17. Alnæs, M. S., Logg, A., Ølgaard, K. B., Rognes, M. E. & Wells, G. N. Unified form language: A domain-specific language for weak formulations of partial differential equations. *ACM Trans. Math. Softw.* **40**, 9:1-9:37 (2014).
18. Ahrens, J., Geveci, B. & Law, C. ParaView: An End-User Tool for Large-Data Visualization. in 717–731 (Elsevier, 2005). doi:10.1016/B978-012387582-2/50038-1.
19. Cahn, J. W. & Hilliard, J. E. Free energy of a nonuniform system. I. Interfacial free energy. *The Journal of chemical physics* **28**, 258–267 (1958).
20. Huston, E. L., Cahn, J. W. & Hilliard, J. E. Spinodal decomposition during continuous cooling. *Acta metallurgica* **14**, 1053–1062 (1966).

21. Planck reveals an almost perfect Universe.

[https://www.esa.int/Science\\_Exploration/Space\\_Science/Planck/Planck\\_reveals\\_an\\_almost\\_perfect\\_Universe](https://www.esa.int/Science_Exploration/Space_Science/Planck/Planck_reveals_an_almost_perfect_Universe).

22. Miville-Deschênes, M. A. *et al.* Planck 2018 results: VI. Cosmological parameters. *Astronomy and Astrophysics* **641**, A6–A6 (2020).

23. Chang, C. *et al.* Dark Energy Survey Year 1 results: curved-sky weak lensing mass map. *Monthly Notices of the Royal Astronomical Society* **475**, 3165–3190 (2018).

24. Umetsu, K. Cluster–galaxy weak lensing. *Astron Astrophys Rev* **28**, 7 (2020).